ENERGETICS OF SIMULATED HCDA BUBBLE EXPANSIONS: SOME POTENTIAL ATTENUATION MECHANISMS

R. J. TOBIN, D. J. CAGLIOSTRO, D. W. PLOEGER

Poulter Laboratory, Stanford Research Institute,
Menlo Park, California 94025, U.S.A.

Realistic predictions of the energetics, or work potential, of hypothetical core disruptive accidents (HCDAs) are a concern in the safety analysis of liquid metal fast breeder reactors (LMFBR). Predictions are currently based on conservative nonmechanistic assumptions concerning the progression of severe core meltdown accidents. Recently, both experiments and analyses have shown that natural attenuation mechanisms such as unsteady and nonequilibrium expansions and flow around internal structures may substantially reduce HCDA energetics. We present experimental results that show these attenuating effects on the work potential of simulated HCDA bubble expansions.

The experiments were conducted in a transparent 1/30-scale model of a typical demonstration-size loop-type LMFBR in which water at room temperature simulated the sodium coolant. Nitrogen gas (100 bars) and flashing water (80 bars) qualitatively simulated sodium vapor and molten fuel expansions. The upper core structure (UCS) simulated an array of empty hexcans, and the upper internal structure (UIS) simulated the control rod and flow guides. The bubble expansions and the motion of the coolant simulant were studied using pressure transducers, water surface displacement gages, and high-speed photography.

Because of its unsteady nature, the nitrogen expansion did not follow a quasi-steady adiabatic expansion even in the absence of internal structures. When the coolant slug impacted the vessel cover, approximately 34% less work was done on the coolant slug than would have been done in a quasi-steady expansion. The addition of a UCS only, a UIS only, and both a UCS and UIS progressively further reduced the peak slug velocity by 7%-52%, the peak axial slug kinetic energy by 15%-78%, the impact pressure on the cover by 17%-51%, and the impact impulse by 11%-27%. With both a UCS and UIS, the peak axial slug kinetic energy was 86% lower than, or 14% of, the ideal quasi-steady expansion work.

Because of the unsteady and nonequilibrium nature of the flashing water expansion, its expansion work in the absence of internal structures was 76% below that expected for a quasi-steady adiabatic expansion. The addition of a UCS only, a UIS only, and both a UCS and UIS progressively further reduced the peak slug velocity by 7%-51%, the peak axial slug kinetic energy by 15%-78%, the impact pressure on the cover by 54%-75%, and the impact impulse by 22%-25%. With both a UCS and UIS, the peak axial slug kinetic energy was 95% lower than, or 5% of, the ideal quasi-steady expansion work.

These experiments show that unsteady core material expansions, the restrictions to the expansion by internal structures, and nonequilibrium effects substantially attenuate the work potential of high pressure bubble expansions. The prototypicality of these results needs to be studied further experimentally and analytically. More prototypic bubble materials may be used in later studies.

* This work is supported by the U.S. Department of Energy, Nuclear Energy Division, Washington, D.C., under Contract No. EY-76-C-03-0115-SX 032.

1. Introduction

LMFBR accidents involving core meltdown are now considered to have the greatest potential for releasing significant amounts of radioactivity to the environment. Such accidents are called core disruptive accidents (CDAs). If a core meltdown could occur, then theoretically, core material motions and interactions might lead to rapid pressure-generation events that could cause structural damage to the reactor and possible release of radioactive materials. The experiments described here were conducted to increase our understanding of the dynamics and thermodynamics of expanding bubbles similar to the CDA bubble in LMFBRs and to aid in developing analytical models for predicting CDA energetics.

2. Attenuation Mechanisms

An important objective of any study of HCDA bubble dynamics should be the identification of physical mechanisms that may result in attenuation of the work potential of an HCDA. The purpose of the experiments discussed here was to study the effects of vessel internal structures on simulated 1/30-scale HCDA bubble expansions [1]. Analysis of these experiments led to identification of three natural attenuating mechanisms: (1) the pressure gradient existing between the lower core and the HCDA bubble within the pool, (2) the nonequilibrium flashing process occurring in the lower core, and (3) the hydrodynamic effects of vessel internal structures. The potential attenuating effects of heat transfer have been discussed by Cagliostro et al. [2].

3. Experimental Apparatus and Instrumentation

The apparatus used to simulate the qualitative features of an HCDA bubble expansion was a simple 1/30-scale model (Figure 1) of the interior of a typical demonstration-size loop-type LMFBR vessel. Included in our model were upper core and upper internal structures. The diameter of the individual flow channels in the upper core structure (UCS) was chosen to closely scale the cross-sectional area of empty subassembly ducts. The UCS consisted of 139 holes, each of 0.152-inch diameter and 2.50 inches long, for a total flow area of 2.52 in^2. Similarly, the upper internal structure (UIS) geometry was linearly scaled to the UIS geometry of a typical demonstration-size loop-type LMFBR. It consisted of 10 holes of 0.332-inch diameter and 19 holes of 0.313-inch diameter for a total flow area of 2.32 in^2. The components in the model were rigid; structural response was not scaled in these experiments. Experiments were performed with and without these structures to clarify their influence on the HCDA bubble expansion.

Sodium coolant was simulated in the model by water at room temperature and atmospheric pressure. The bubble sources simulating the expansion of sodium vapor and molten fuel were contained in the lower core shown in Figure 1. Both high-pressure nitrogen gas and high-pressure flashing water were used as bubble sources. After the appropriate initial conditions were established within the lower core and acrylic vessel, the experiments were initiated at $t = 0$ by detonating an explosive to open the sliding doors. The flow path between the lower and upper cores began to open at $t = 1.2$ msec and took 230 μsec to fully open. The expansion of the gas or flashing liquid contained in the lower core then drove the liquid coolant out of the upper core and formed within the coolant pool an expanding bubble, which drove the coolant pool to impact on the vessel cover.

The experiment instrumentation is shown schematically in Figure 1. Pressures in the lower core, upper core, within the pool and bubble, and at the vessel cover as well as surface displacement of the pool were recorded on both oscillograms and magnetic tape. Quartz piezoelectric pressure transducers were used in the lower core, upper core, and cover. Those in the lower core were water cooled. The pressure in the pool was measured using a waterproof 3/8-inch-diameter, four-element Tourmaline pressure transducer. Two conductance-type gages were mounted in the bottom of the cover to measure the displacement of the water surface. The bubble expansion was recorded by a Hycam Model 41-004 camera at a nominal speed of 10,000 frames per second.

4. Discussion of Experiments and Results

4.1 Effects of Pressure Gradient

The nitrogen source experiments illuminate the dynamic features of the bubble expansion without the complications of heat transfer and phase change. Experiments were conducted with the internal structures present in various combinations. The experiments conducted and the results of these experiments are summarized in Table I. The nitrogen source was initially at 100 bars and room temperature. In the experiments without internal structures, as the sliding doors separating the lower and upper cores begin to open, the nitrogen gas begins to accelerate the upper core and pool fluid. As this fluid begins to move, the thin viscous layer on the wall of the upper core is convected into the pool and rolls up into a vortex ring at the top of the upper core barrel. The bubble rising within the upper core contains a large volume of water with entrainments of about 80%. This entrainment is believed to result from the early instability of the accelerating gas-liquid interface and the associated mixing. As the bubble emerges into the pool, it soon engulfs the vortex located just above the upper core. Although the percentage entrainment in the bubble falls (to ∿25% at slug impact) as the bubble expands, the entrained mass increases. This entrainment probably takes place at the sides of the bubble in association with the dissipating vortex. The axial bubble velocity is greater than the axial pool velocity and the bubble grows radially until slug impact. Slug impact occurs when the pool displaces the initial cover gas volume and impacts the vessel cover. A typical slug impact pressure record (Figure 2) shows several pulses, which occur as the water surface recoils off the vessel cover following slug impact and then reimpacts the cover as the core gas reexpands. The impulses shown in Table I were calculated for the first pulse over an 0.8-msec interval beginning at a 90% compression of the cover gas.

During the expansion to slug impact, a pressure gradient exists between the lower core and the bubble within the pool. This gradient informs us that the expansion process is not quasi-static. The pressure doing work on the coolant slug is the pressure acting at the gas-liquid interface of the expanding bubble. This interface is established as the sliding doors open and then moves past the upper core and bubble pressure transducers as the bubble expands. The pressure at this interface is determined from pressure records taken at specific locations within the apparatus. Figure 3(a) shows lower core, upper core, and pool and bubble pressure measurements for the nitrogen source experiment with no internal structures. Those portions of these pressure records that best characterize the interface pressure are assembled into the composite shown in Figure 3(b).

The expansion work done by the source in driving the coolant pool upward until it impacted on the vessel cover (the integral of the product of the composite pressure and the differential volume displaced by the pool) was 2.98 kW-sec. This is approximately 66% of that expected in an ideal quasi-static expansion. The peak slug kinetic energy should approximate this work done on the slug by the bubble source if there are no significant energy losses and few turbulent or rotational motions. The peak kinetic energy of the slug can be estimated by assuming that all the coolant liquid above the top of the upper core moves at the velocity of the water surface. Support for this simple method of calculating the slug kinetic energy comes from predictions of these experiments made at LASL using the SIMMER II computer code [3]. The average value of the peak slug kinetic energy for experiments D-006 and D-002 is 2.85 kW-sec, which is within 4% of the expansion work done on the slug by the bubble source, as discussed above. Since the expansion work done by the source and the slug axial kinetic energy are about equal, we conclude that, in the absence of internal structures, the coolant slug moves with little energy loss or turbulence production in response to the work done on it by the bubble source.

A scaling analysis of the nitrogen source experiments, based on the significant physical parameters, was conducted. Our concern was whether the dynamic phenomena present in a nitrogen source experiment at 1/30-scale would be present to the same degree in a full-scale experiment using the same materials and initial conditions. This includes such features as the bubble shape, the percentage entrainment in the upper core and bubble, and the slug impact pressure. The only dimensionless parameters that have different values at 1/30- and full-scale are the Reynolds and Weber numbers. Since both of these numbers are large at either scale, viscous and surface tension forces will not have a significant influence on the macroscopic dynamic features of the bubble expansion; thus these features scale.

4.2 Nonequilibrium Effects

The flashing water source experiments were more complex than the nitrogen source experiments because of the presence of heat transfer and phase change phenomena. Experiments were conducted with the same combinations of internal structures that were studied with the nitrogen source. The flashing source contained saturated liquid at initial conditions of 80 bars and 563°F. Results from the flashing source experiments are summarized in Table II. A typical slug impact pressure record is shown in Figure 4. The impulses shown in Table II were calculated for the first slug impact pulse over a 1.0-msec interval beginning at a 90% compression of the cover gas. The experiment without internal structures proceeded in a manner quite similar to that described above for the nitrogen source. However, pressure histories in the lower core, upper core, and bubble were of a different character.

Pressure records typical of the flashing source experiment with no internal structures are shown in Figure 5(a). An explanation of the character of the lower core pressure record typical of the flashing source is found in nonequilibrium thermodynamics. When the sliding doors are opened, an expansion wave travels into the lower core and reduces the pressure. This reduction in pressure supersaturates the lower core liquid, resulting in a metastable state, and vapor formation begins in an attempt to restore equilibrium. Formation of vapor bubbles requires that heat be extracted from the liquid adjacent to the bubble and invested as heat of vaporization in the forming vapor. Thus, the vapor and

adjacent liquid are cooler than the bulk liquid, and a thermal nonequilibrium exists. The pressure in the flashing liquid drops to the saturation pressure corresponding to the temperature of the cooled liquid adjacent to the vapor bubble.

The 1/30-scale flashing water expansions are not equilibrium expansions because the time for the expansion, τ, is short compared with the time for the temperature and pressure of the water to reach equilibrium, t_r, i.e., $\tau/t_r \ll 1$. Therefore, the nonequilibrium effects observed in the 1/30-scale experiments would be expected to occur at full-scale if the ratio τ/t_r is also less than one at full scale. The actual value of τ/t_r in either small or large scale experiments will determine the fraction of the equilibrium work that is done in moving the coolant slug. It is, therefore, the equilibrium, or "relaxation," time (t_r) that we need to be able to predict analytically or measure experimentally before we can predict the behavior of expansions of prototypic materials at full-scale. Experimental support for a nonequilibrium expansion model would provide a strong basis for the understanding and choice of a prototypic source simulant material. Because the nonequilibrium nature of the flashing source expansion results in a lower-core pressure below the pressure that would occur during an equilibrium expansion, the source expansion work is less than the ideal work potential of the flashing source.

As in the nitrogen experiments, a pressure gradient exists between the lower core and the bubble within the pool; therefore, the pressure acting on the coolant slug is not well represented by the lower core pressure. This gradient may be due to unsteady or two-phase phenomena such as choking in the flow path between the lower core and the pool. The pressure acting on the coolant slug is estimated to be that shown in Figure 5(b).

The expansion work calculated using the composite pressure is lower than the work expected in an ideal quasi-static expansion because of the two attenuation mechanisms: (1) the 400-psi or 40% reduction in lower core pressure due to nonequilibrium effects and (2) the further 300-psi or 50% reduction due to the pressure gradient between the lower core and the gas-liquid interface of the expanding bubble. The calculated expansion work done by the source in driving the coolant pool upward until it impacted the vessel cover was 1.3 kW-sec. This is approximately 25% of that expected in an ideal quasi-static expansion and compares with a peak slug kinetic energy of 1.26 kW-sec based on the assumption that all the liquid above the top of the upper core is moving at the coolant water surface velocity.

The behavior of flashing source experiments at full-scale is not currently understood because of questions about the nonequilibrium and two-phase phenomena present in the 1/30-scale flashing source experiments. Experiments are being planned at SRI to address these questions and to identify other simulant materials that might behave in a manner more typical of the core materials in a prototype LMFBR.

4.3 Effects of Internal Structures

Internal structures attenuate the slug impact energy by increasing the time to slug impact, reducing the slug impact velocity, and reducing the peak pressure and impulse on the vessel cover. The upper core structure tested caused the smallest change in response, and the presence of both structures caused the greatest change. The apparent mechanisms that produce this result are throttling and the diversion of a portion of the gas or vapor work from the production of axial motion to the production of organized rotational motion

(in the form of vortices) and random turbulent motion. The effects of internal structures on the primary slug impact pulse are shown for both bubble sources in Figures 6(a) and (b). The effects on the peak pool surface velocity, peak pool slug kinetic energy, peak cover pressure, and slug impact impulse are summarized for both bubble sources in Table III.

5. Summary

Each of the three attenuation mechanisms discussed, (1) the pressure gradient between the lower core and the expanding bubble, (2) the nonequilibrium nature of the flashing source expansion, and (3) the effects of internal vessel structures, results in reductions in the coolant slug kinetic energy from the ideal quasi-static work potential of the bubble source. The overall results of these experiments are summarized in Table IV.

References

[1] TOBIN, R. J., CAGLIOSTRO, D. J., "Effects of Vessel Internal Structures on Simulated HCDA Bubble Expansions," Technical Report 5, SRI Project PYU-3929, SRI International, Menlo Park, CA (November 1978).

[2] CAGLIOSTRO, D. J., FLORENCE, A. L., ABRAHAMSON, G. R., NAGUMO, G., "Characterization of an Energy Source for Modeling Hypothetical Core Disruptive Accidents in Nuclear Reactors," Nuclear Engineering and Design, Vol. 27, No. 1 (March 1974).

[3] BELL, C. R., et al., "SIMMER-II Analysis of LMFBR Post-Disassembly Expansion," Proceeding of the ENS/ANS International Topical Meeting on Nuclear Power Reactor Safety, Brussels, Belgium, 16-19 October 1978.

Table I

SUMMARY OF EXPERIMENTAL RESULTS, NITROGEN BUBBLE SOURCE

Expt. No.	Internal Structures Present	Initial Gap (inches)	Slug Impact Time (msec from doors begin to open)	Peak Cover Pressure[a] (psi)	Impulse of First Slug Impact Pulse (lb_f-sec)	Peak Surface Velocity[b] (in/msec)	Peak Slug Kinetic Energy[c] (kW-sec)
D-002	None	1.02	2.20	5310	67.0	1.12	3.24
D-006	None	0.91	2.16	4753	66.6	0.97	2.46
D-003	UCS Only	0.99	2.51	4095	59.4	0.97	2.42
D-005	UIS Only	0.90	2.75	2960	43.3 8.8 (UIS impulse)	0.59	0.85
D-004	UCS + UIS	0.81	2.84	2462	40.0	0.50	0.61

[a] Average value for each experiment.
[b] The value at slug impact of the derivative of a polynomial fit to the average water surface displacement gage measurement.
[c] Based on the peak surface velocity and the total mass of liquid contained in the pool above the top of the upper core.

Table II

SUMMARY OF EXPERIMENTAL RESULTS, FLASHING WATER BUBBLE SOURCE

Expt. No.	Internal Structures Present	Initial Gap (inch)	Slug Impact Time (msec from doors begin to open)	Peak Cover Pressure[a] (psi)	Impulse of First Slug Impact Pulse (lb_f-sec)	Peak Surface Velocity[b] (in/msec)	Peak Slug Kinetic Energy[c] (kW-sec)
E-001	None	0.89	3.10	2325	41.9	0.67	1.26
E-002	UCS Only	0.90	3.43	1667	32.5	0.62	1.07
E-004	UIS Only	0.91	3.86	1082	24.3 13.2 (UIS impulse)[d]	0.42	0.46
E-003	UCS + UIS	0.92	4.41	668	18.3 13.2 (UIS impulse)[d]	0.37	0.33

[a] Average value for each experiment.
[b] The value at slug impact of the derivative of a polynomial fit to the average water surface displacement gage measurement.
[c] Based on the peak surface velocity and the total mass of liquid contained in the pool above the top of the upper core.
[d] Composite based on Experiments E-003 and E-004.

Table III

SUMMARY OF THE EFFECTS OF INTERNAL VESSEL STRUCTURES

INTERNAL STRUCTURE(S)	REDUCTION COMPARED WITH NO INTERNAL STRUCTURES Peak Surface Velocity	Peak Slug Kinetic Energy	Peak Cover Pressure	Slug Impact Impulse
Nitrogen Bubble Source				
UCS[a] Only	7%	15%	19%	11%
UIS[b] Only	44%	70%	41%	35%[c] 22%[d]
Both UCS + UIS	52%	79%	51%	40% 27%
Flashing Water Bubble Source				
UCS Only	7%	15%	28%	22%
UIS Only	37%	63%	54%	42% 11%
Both UCS + UIS	45%	74%	71%	56% 25%

[a] Upper Core Structure.

[b] Upper Internal Structure.

[c] Impulse based on the slug impact pressure.

[d] Impulse based on the slug impact pressure and the additional load applied to the cover through the UIS columns.

Table IV

AXIAL SLUG KINETIC ENERGY
AS A PERCENTAGE OF THE IDEAL QUASI-STATIC
WORK POTENTIAL OF THE BUBBLE SOURCE

Bubble Source	Without Internal Structures	With Upper Core and Upper Internal Structures
Nitrogen	66%	14%
Flashing water	24%	5%

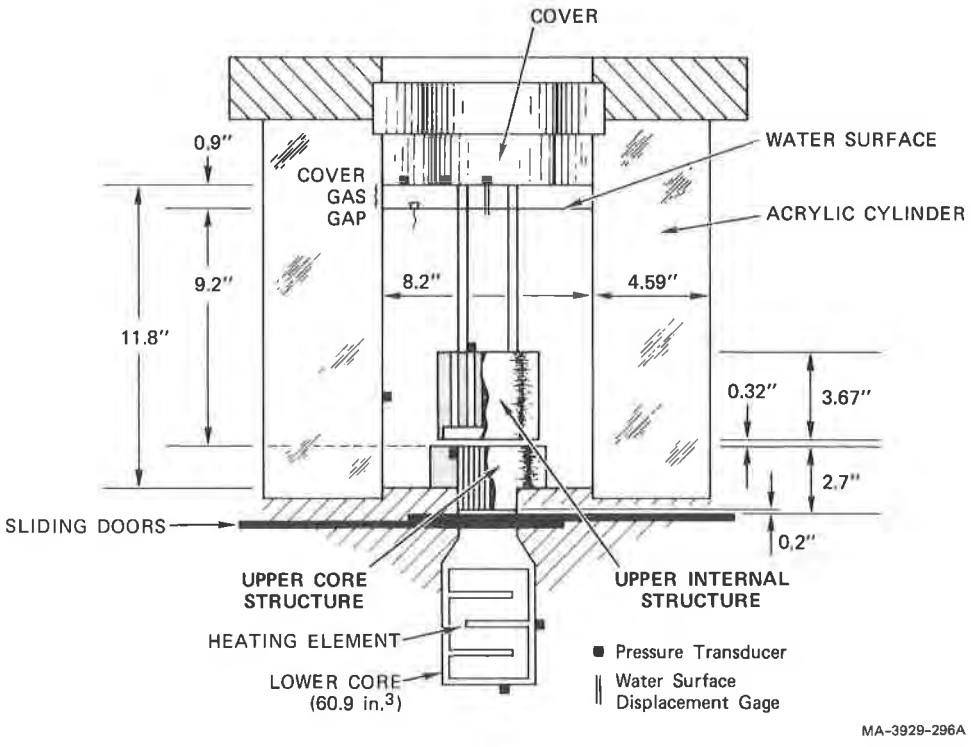

FIGURE 1 1/30-SCALE VESSEL AND INSTRUMENTATION

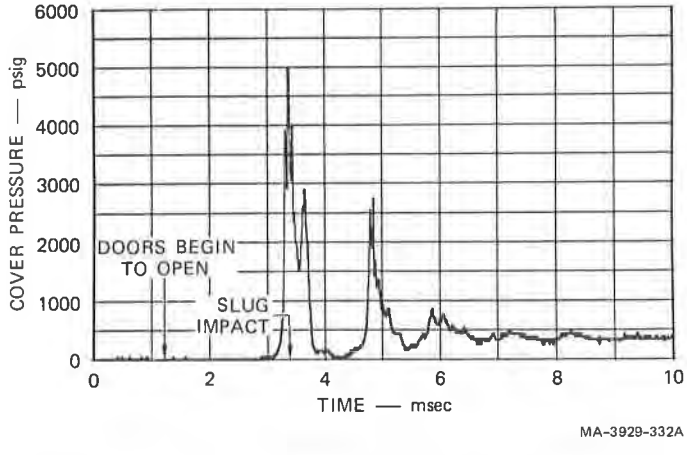

FIGURE 2 TYPICAL COVER PRESSURE, EXPERIMENT D-006 (NO INTERNAL STRUCTURES), NITROGEN BUBBLE SOURCE

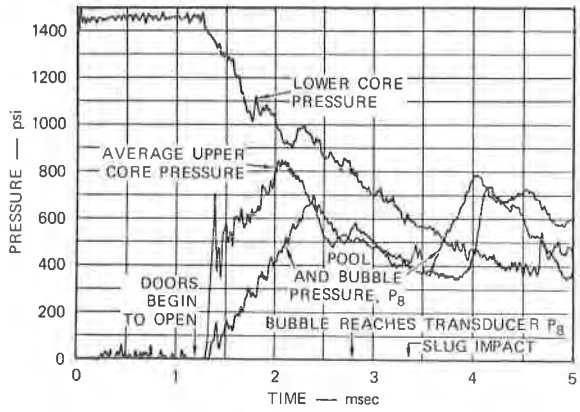

(a) VESSEL PRESSURES

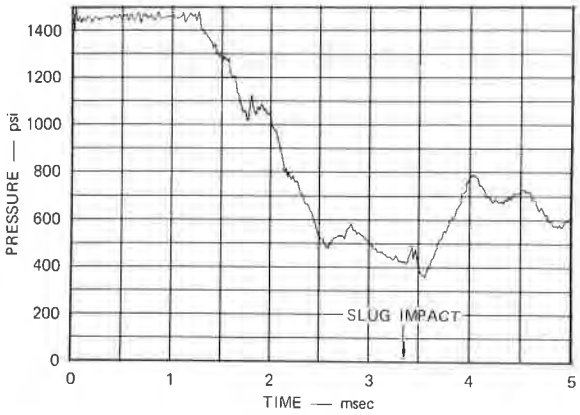

(b) BEST ESTIMATE OF THE PRESSURE ACTING AT THE GAS-LIQUID INTERFACE OF THE COOLANT SLUG

MA-3929-372A

FIGURE 3 PRESSURE ACTING AT THE BUBBLE INTERFACE OF THE COOLANT SLUG, EXPERIMENT D-006 (NO INTERNAL STRUCTURES), NITROGEN BUBBLE SOURCE

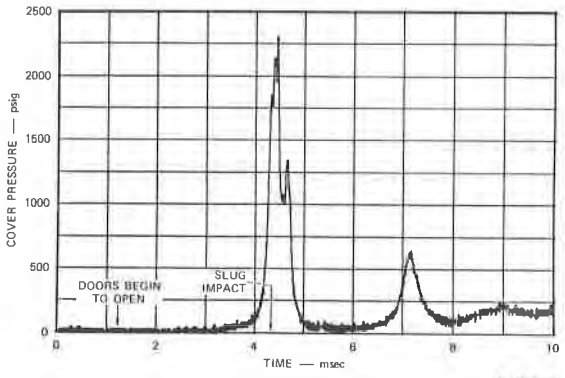

FIGURE 4 TYPICAL COVER PRESSURE, EXPERIMENT E-001 (NO INTERNAL STRUCTURES), FLASHING WATER BUBBLE SOURCE

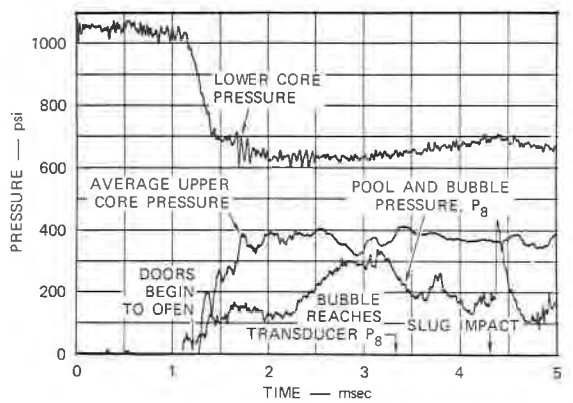

(a) VESSEL PRESSURES

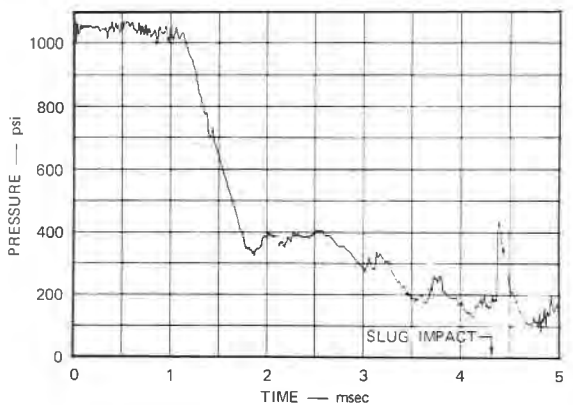

(b) BEST ESTIMATE OF THE PRESSURE ACTING AT THE VAPOR-LIQUID INTERFACE OF THE COOLANT SLUG

MA-3929-373A

FIGURE 5 PRESSURE ACTING AT THE BUBBLE INTERFACE OF THE COOLANT SLUG, EXPERIMENTS E-001 AND C-007 (NO INTERNAL STRUCTURES), FLASHING WATER BUBBLE SOURCE

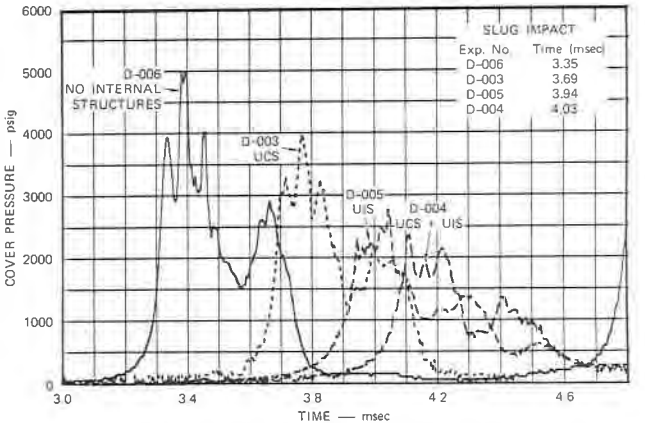

(a) NITROGEN BUBBLE SOURCE

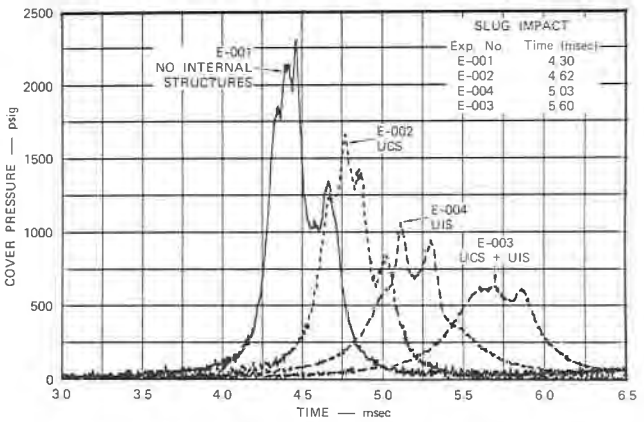

(b) FLASHING WATER BUBBLE SOURCE

FIGURE 6 EFFECT OF INTERNAL STRUCTURES ON THE FIRST SLUG IMPACT PRESSURE PULSE